



OXFORD CENTRE FOR COLLABORATIVE APPLIED MATHEMATICS

Report Number 10/64

**Hot Charge Pairs and Charge Generation in Donor Acceptor  
Blends**

by

**James Kirkpatrick**



Oxford Centre for Collaborative Applied Mathematics  
Mathematical Institute  
24 - 29 St Giles'  
Oxford  
OX1 3LB  
England



## Hot Charge Pairs and Charge Generation in Donor Acceptor Blends

James Kirkpatrick<sup>1, a)</sup>

*Department of Physics, Oxford University, Parks Road, Oxford OX1 3LB,  
UK*

In organic photovoltaic cells, charge generation takes place in two phases: first excitons are split by donating an electron to an electron acceptor, second the charge pair, strongly bounded by Coulomb forces, must separate before it can recombine. In this paper we suggest that overcoming the Coulomb binding is possible because the vibrational mode excited by exciton splitting is also coupled to charge hopping. This insight provides a model for how excess driving force for exciton splitting can aid charge transfer, so long as vibrational relaxation is slow compared to charge transfer. The model predicts an approximately linear dependence of charge yield on the driving force for exciton splitting. It also shows that high yields can be achieved with the observed fast rates of recombination. It also provides a molecular basis for understanding thermalization in donor acceptor blends. In the limit of slow internal vibrational relaxation (compared to charge hopping), we provide a rule of thumb to predict the thermalization distance in this hopping regime:  $d = a \log_2 \left( \frac{\Delta G}{\hbar\omega} \right)$ , where  $a$  is the separation between molecules,  $\Delta G$  is the driving force for charge separation (including Coulomb binding) and  $\hbar\omega$  is the vibrational energy of the acceptor mode.

Keywords: charge generation, solar cell, electron phonon coupling

---

<sup>a)</sup>Electronic mail: kirkpatrick@maths.ox.ac.uk

## I. INTRODUCTION

In an organic blend, charges are generated by splitting excitons at the interface between materials with different electron affinities: the donor material is typically responsible for absorbing light and has a greater affinity for holes; the acceptor has greater affinity for electrons. In order to generate a photocurrent, charges must escape each other's Coulomb attraction without recombining. Exciton splitting is typically driven by a large ( $> 0.5$  eV) driving force<sup>1</sup>. We develop a model where this excess energy aids escape from the Coulomb well. This can happen because the polaron pair formed by exciton splitting is in a vibrational excited state. The mode excited is the superposition of the modes that change the donor from the exciton to the charged geometry and the acceptor from the neutral to the charged geometry. This second mode is also coupled to charge transfer in the acceptor molecule, hence, the states formed just after exciton splitting are able to diffuse more rapidly. In other words, the exciton's excess energy can be stored in the vibrational modes of the polaron and can be used to help escape the Coulomb attraction.

That hot states are involved in charge separation is not a new idea. Peumans *et al.* need to assume very large thermalization radii to reproduce experimental charge yields<sup>2</sup>. Models involving hot excitons have been used to describe charge generation in pure polymers<sup>3</sup>. Models by Offermans *et al.* predict increased charge yields if charges are generated hot<sup>4</sup>. Experiments have also shown that charge mobilities are higher immediately after charge generation<sup>5</sup>, suggesting that charge transfer is fastest immediately after exciton splitting. However, *how* thermalization lengths are connected to molecular properties is not yet understood.

Understanding the link between the driving force for charge separation and quantum yield will help determine the limiting efficiency of organic solar cells (OSC). OSCs can have high quantum efficiencies<sup>6</sup>, however open circuit voltages (Voc) are still substantially smaller than the band gap. The Voc for several materials is less than half the maximum of external quantum efficiencies<sup>1</sup>. Until recently, designing better OSC materials was thought to require reducing the energy lost in exciton splitting<sup>7</sup>. Recent measurements by Okhita *et al.*<sup>8</sup> show that reducing the energy loss also reduces the yield of charges: bad news for OSC as increasing the Voc would also lower short circuit current.

Another significant problem is that modeling simulations of charge generation routinely

use recombination timescales in the microsecond range<sup>4,9-11</sup> in order to achieve high yields of charges ( $> 10\%$ ), whereas experimental measurements of the rate of charge recombination have found it to be faster than nanoseconds<sup>12-14</sup>. In this paper high yields are obtained with fast recombination by including the effect of charge transfer from hot states.

The key insight presented in this paper is that the vibrational mode excited by exciton dissociation *must* always facilitate charge transfer. Traditional charge transfer rate equations, such as those from Marcus theory, assume that thermalization is immediate upon charge transfer. In this work we develop a rate expression which can keep track of the number of phonons before and after charge transfer, allowing to model the competition between vibrational relaxation and hot transfer. Since only antisymmetric combinations of localised modes contribute to charge transfer, at each charge transfer step the available vibrational energy is reduced. Therefore there are two ways for the polarons to lose vibrational energy exist: internal vibrational relaxation (the vibrational state changes with no accompanying change in electronic state) and charge transfer (the electronic part of the polaron wavefunction moves spatially, leaving some of the vibrational excitation behind).

Figure 1 shows the processes modeled in the paper. Each column of energy levels represents an electronic state, labeled by the distance  $d$  between electron and hole. At a distance 0 the system is in the neutral ground state (black energy levels) or in the excited state (red energy level). The processes competing are: i) exciton dissociation; ii) charge transfer from a vibrationally excited state; iii) decay of the vibrational energy by internal conversion; and iv) charge recombination to the ground state. Exciton splitting is not modeled explicitly, but is used to provide the initial excited vibrational state.

The theory of charge transfer between isolated electronic states including quantum vibrations has been looked at extensively in the past twenty years<sup>15-17</sup>. A less well understood class of problems involves charge transfer between multiple electronic states. Charge transport in DNA is the best studied problem of that class to have been analysed theoretically<sup>18</sup>, although recently work has been done on understanding charge transport in the condensed phase in organic crystals<sup>19,20</sup>, in discotic liquid crystals<sup>21</sup> and in conjugated polymers<sup>22</sup>. In their pioneering work on DNA, Jortner and coworkers distinguish two main cases: long-range unistep charge transfer and multi-step incoherent hops. The two cases are distinguished by the value of the transfer integrals between the electronic states, if the electronic coupling is sufficiently strong it is possible for charges to tunnel through several electronic states

(known as "bridge states") before localising in a process known as super-exchange coupling. Crucially the bridge states must be near degenerate. In the limit of weaker coupling charges localise at each hop; most of the afore-mentioned work on transport in the condensed phase takes place in this limit. In this paper we introduce a new regime: the couplings are assumed to be small enough that transport occurs by hopping, but large enough that hopping competes with vibrational relaxation. The assumptions of the model are therefore similar to those of the non-adiabatic Marcus-Levich-Jortner equation (i.e. that the transfer integrals weighted by appropriate Franck-Condon factors are small compared to the outer sphere reorganization energy), but to those we add the requirement that vibrational relaxation occurs on a similar time scale to charge transfer and that the phase coherence of the wavefunction is lost at each hop. In addition to these theoretical assumptions, the model is implemented on a one dimensional lattice, including coupling of each electronic state to one vibrational mode only and disregarding diagonal or off-diagonal disorder. These are rather crude approximations, but they are sufficient to elucidate the mechanism by which nuclear vibrations allow the excess electronic energy of the exciton to be used to escape the Coulomb attraction of polarons.

## II. THEORY

Traditional charge transfer theories are inadequate at describing the competition between charge transfer and thermalization because relaxation of bath modes is assumed to be faster than all other processes: thermalization is assumed to be immediate. Our aim is to obtain a rate equation for charge transfer between two electronic states  $|i\rangle$  and  $|j\rangle$  each coupled to a quantum mode and to a classical bath. We assume that the quantum mode is not thermalized, but that the classical bath is thanks to its large size. Assuming non-adiabatic conditions, the rate of going from electronic state  $|i\rangle$  to  $|j\rangle$  and changing the antisymmetric combination of modes from  $a$  to  $a'$ , the rate is:

$$\Gamma(i, a \rightarrow j, a') = \frac{J_{i,j}^2}{\hbar} \sqrt{\frac{\pi}{\lambda_o kT}} \langle a|a'\rangle^2 \exp\left(-\frac{(\Delta G_{i,j} + \lambda_o + \hbar\omega(a' - a))^2}{4\lambda_o kT}\right) \quad (1)$$

where  $\lambda_o$  is the outer sphere reorganization energy and  $\Delta G_{i,j}$  the difference between the electronic state energies. The derivation of this equation closely follows Jortner's work and is repeated in the supplementary information<sup>23</sup>, with the aim of emphasizing the importance of the antisymmetric vibrational modes.

There is an important consideration to make when moving from a system with only two molecules to one with more. When charge transfer occurs between two electronic states  $i$  and  $j$ , only the antisymmetric modes of the oscillators coupled to each of those two states are able to change. However, the symmetric combinations cannot be ignored since once the system is ready to hop again from state  $j$ , it will be necessary to construct the antisymmetric combination of modes related to state  $j$  and whatever state the system may be hopping to. This is not merely a technicality, it ensures that when the polaron hops only part of the vibrational energy is carried with it. Therefore, if the mode associated with electronic state  $i$  changes in nuclear state  $\mu$  to  $\rho$  and the mode associated to  $j$  changes from  $\nu$  to  $\sigma$ , the rate of charge transfer can be written as:

$$\Gamma(i, \mu, \nu \rightarrow j, \rho, \sigma) = \sum_{A', A} P(S, A | \nu, \mu) \Gamma(i, A \rightarrow j, A') P(S, A' | \rho, \sigma) \quad (2)$$

The probability terms  $P(S, A | \mu, \nu)$  represent the probability of a system of two simple harmonic oscillators in localised modes  $\mu$  and  $\nu$  to be in a symmetric mode  $S$  and an anti-symmetric mode  $A$ . By using a probability term, rather than explicitly considering the wavefunction, we implicitly assume that with each charge hop, coherence is lost.

The probabilities  $P(S, A | \mu, \nu)$  can be determined by assuming that the ladder operators for the symmetric/antisymmetric modes are given by combinations of the appropriate localised ladder operators  $a_1^\dagger$  and  $a_2^\dagger$ :  $a_{s/a}^\dagger = \frac{a_1^\dagger \pm a_2^\dagger}{\sqrt{2}}$ . The amplitude of the projection of such a state into the corresponding localised modes is:

$$P(S, A | \mu, \nu) = 2^{-(\mu+\nu)} \left( \sum_{\substack{0 \leq m \leq \mu \\ 0 \leq n \leq \nu}} (-1)^{n-\nu} \binom{\mu}{m} \binom{\nu}{n} \sqrt{\frac{(m+n)!(\mu+\nu-m-n)!}{\mu!\nu!}} \delta(S, (m+n)) \delta(A, (\mu+\nu-m-n)) \right)^2 \quad (3)$$

where the  $\delta$  functions ensures that the probability is non-zero only if  $\mu + \nu = A + S$  (proof in the supplementary information<sup>23</sup>).

Having an equation which keeps track of process (ii) from figure 1, it is possible to study the competition with vibrational relaxation (process iii) by also introducing a rate for vibrational relaxation:

$$\Gamma(i, a \rightarrow i, a - 1) = k_{VR} \quad (4)$$

Charge recombination (process (iv)) can also be modelled using equations 1-3, as it is simply another charge transfer process.

We do not explicitly model exciton dissociation, but use the parameters for exciton dissociation to determine the probability of starting the simulation from a particular vibrational level  $\nu$ :

$$P(\nu) = \sum_A \frac{\Gamma(0^*, 0 \rightarrow 1, A)}{\sum_{A'} \Gamma(0^*, 0 \rightarrow 1, A')} P(S, 0 | A - \nu, \nu) \quad (5)$$

where each term in the summation represents the probability of producing a certain anti-symmetric state  $A$  and the probability that the state gives rise to localised state  $\nu$ . The excited neutral state is labeled  $0^*$ . Note that this expression depends on the difference in energy between the excited state and the first charged state (labelled  $\Delta G$  in 1), on  $\lambda_o$ , on the Huang Rhys factor and on  $\hbar\omega$ , but not on the matrix element.

The linear dynamical system defined by these equations is solved by generating a starting state vector  $|1, \nu\rangle$  and updating it using a continuous time random walk algorithm<sup>24</sup>. Rates are then computed only for states as they are needed. The simulation is stopped if either the charges recombines, or if they reaches a certain distance  $d$ . We apply this model it to a one dimensional chain of acceptors, with the positive polaron immobilised at one end of the chain. Electronic states are uniquely labeled by the distance between hole and electron  $|i\rangle$ , for example state  $|1\rangle$  will have the electron and hole one lattice apart spacing. State  $|0\rangle$  is the neutral ground state reached if the electron and hole recombine. Each state  $|i\rangle$  is connected to its neighbors  $|i + 1\rangle$  and  $|i - 1\rangle$  with the same transfer integral for charge separation  $V_{CS}$ , with the exception of states  $|1\rangle$  and  $|0\rangle$ , which are connected by the transfer integral for charge recombination  $V_{CR}$ . This allows the timescales for charge transfer and recombination to be controlled independently.

The energy  $E(i)$  of a particular electronic state  $|i\rangle$  is determined only by the applied electric field  $F$  and the Coulomb potential:  $E(i) = -\frac{e^2}{4\pi\epsilon_0\epsilon a i} - F a i$ , where  $a$  is the lattice

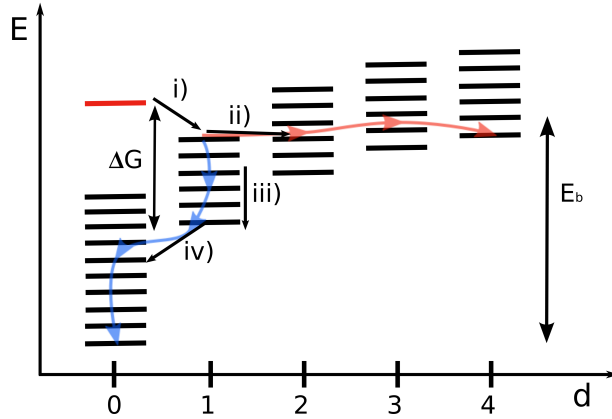


FIG. 1. Sketch of the mechanisms described in the main text: i) exciton splitting, ii) charge transfer from a vibrational excited state, iii) internal vibrational relaxation, iv) recombination. The red arrow is a trajectory leading to charge generation whereas the blue one to recombination. The pseudo bandgap  $E_b$  and the driving energy for exciton splitting  $\Delta G$  are shown.

constant,  $\epsilon$  and  $\epsilon_0$  are respectively the relative and vacuum permittivities and  $e$  is the charge of an electron. The energy of state  $|0\rangle$  is a fixed value  $E_b$  below the zero of this potential.  $E_b$  is the the pseudo band gap between the highest occupied molecular orbital of the donor and the lowest unoccupied molecular orbital of the acceptor.  $E_b$  and  $\Delta G$  (the driving force for exciton splitting) are shown schematically in 1.

### III. RESULTS

All the modeling in the rest of this paper uses the following parameters for the energetics:  $a = 1 \text{ nm}$ ,  $E_b = -0.9 \text{ eV}$ ,  $\epsilon = 4$  and  $F = 5 \cdot 10^5 \text{ V/cm}$ . The electric field employed is rather large, smaller fields would be necessary if more subtle models of the polarization of the interface<sup>25,26</sup> lowering the barrier to charge separation, or if a three dimensional model which allowed both charges to move was employed<sup>9,11</sup>, or if a three dimensional simulation was carried out (because of the greater effect of entropy). As argued later on, this large electric field is necessary to obtain reasonable charge yields within our simple model, but it is independent of the thermalization distance. The parameters of the charge transfer equation used are: the Huang-Rhys factor  $\Delta = 1$ ,  $\hbar\omega = 0.17 \text{ eV}$ ,  $\lambda_o = 0.1 \text{ eV}$ ,  $V_{CS} = 0.05 \text{ eV}$ , and

$k_{VR} = 10^{12} \text{ s}^{-1}$ , a set of values typical for fullerene<sup>27</sup>. The parameters for recombination are the same as above, but with a transfer integral  $V_{CR} = 0.01 \text{ eV}$ . This puts the recombination rate in the picosecond regime, with the exact value depending on which vibrational level the system is recombining from. Since there is a considerable amount of uncertainty on the values of these parameters, they will be systematically varied to determine their relative importance.

Panel a) in figure 2 shows the conditional probability of the system reaching a certain distance  $d$  given that it has already reached a distance  $d - 1$  for different numbers of initial vibrational quanta. Showing the conditional probability helps identify the thermalization distance, because once the system thermalizes all the curves fall onto each other: the initial number of vibrational quanta is, in other words, forgotten. Increasing the number of phonons in the initial state massively increases the probability that the charge is able to escape recombination, for example in the vibrational ground state the probability of recombining immediately is 60%, but with just one quantum of vibrational energy this probability decreases to less than 1%. Simulations with one extra phonon thermalise after just one hop. The higher excited states thermalise at a distance of approximately 4nm. The inset of panel a) shows the probability of a particular vibrational excited state being created given a certain  $\Delta G$ . Clearly highly excited states are more likely for greater  $\Delta G$ . The excited state  $n_q$  which is most likely to be generated is approximately when  $n_q = \left(\frac{\Delta G}{2\hbar\omega}\right)$ . Assuming charge transport is much faster than recombination, all the thermalization will be due to hopping. In this case, the number of hops  $n$  necessary to thermalize the system is  $2^n = n_q$ . In other words, at each step half of the vibrational energy is left behind. This approximate equation matches reasonably well with our simulations: when we start the simulation with 5 phonons,  $\log_2(5) = 2.3$ , *i.e.* thermalization will occur between the second and third hop, in reasonable agreement with our simulations. If recombination was sufficiently slow that it could not occur before thermalization, we could use this thermalization distance as the initial distance between charges in a traditional model of charge separation. For a donor acceptor heterojunction characterised by the above constants, this would suggest a thermalization distance of 3.6 nm, in good agreement with the distance is that Peumans et. al.<sup>2</sup> assume to explain charge separation in donor acceptor bilayers. It is importante to note that this estimate of the thermalization distance depends only on the initial number of phonons  $n_q$  and not on the electric field or other physical parameters.

If we allow charges to recombine before thermalization, simulation of the competition of the different processes is required. The charge yield can be obtained by weighing the probabilities of reaching a certain distance without recombining by the probability that that starting number of phonons is achieved for a certain  $\Delta G$ . This allows to determine the charge yield at a certain distance as a function of  $\Delta G$ . Panels b),c) and d) show the effect on charge yield at 5 nm as a function of  $\Delta G$  of: the transfer integrals for charge transport (b), the rate of vibrational relaxation (c) and  $\lambda_o$  for charge transport (d). The yield of charges is the result of competition of three basic process: charge transport, internal vibrational relaxation and charge recombination. Decreasing the transfer integral not only reduces the yield of charges, it also decreases the dependence of yield on  $\Delta G$ . This is because slowing down charge transfer not only makes recombination more likely (reducing the yield) it also makes vibrational relaxation faster (reducing the dependence on  $\Delta G$ ). Increasing the rate of vibrational relaxation reduces the yield because it causes relaxation to occur faster.  $\lambda_o$  has a large effect because it dictates how much energy is lost to the classical bath with each hop: making it larger makes the system thermalise more effectively through charge transfer. Note that the dependence of charge yield on initial driving force is approximately linear. This makes sense if we realise that the probability of dissociation will be approximately exponential in the attraction of charges after thermalization, since the thermalisation distance itself depends logarithmically on  $\Delta G$ , we would expect a weak dependence of the charge yield with the driving force.

#### IV. CONCLUSION

Three conditions must be fulfilled for vibrational excitation to aid charge generation : 1) the vibrational mode excited by exciton splitting must be the same as that coupled to charge separation, 2) vibrational relaxation must be slow compared to charge tunneling, 3)  $\lambda_o$  must be small to ensure low losses to the classical bath. The key insight of this paper is that condition 1) is *always* true for the acceptor molecule. If, however, the modes that lead to exciton splitting are not orthogonal to those coupled to charge transfer also in the donor molecule, the effect of the initial energy would be increased. This might provide a rationale for why donor-acceptor copolymers seem to be able to generate higher quantum yields with a smaller loss in energy<sup>28</sup>: possibly the geometric relaxation in a cation and

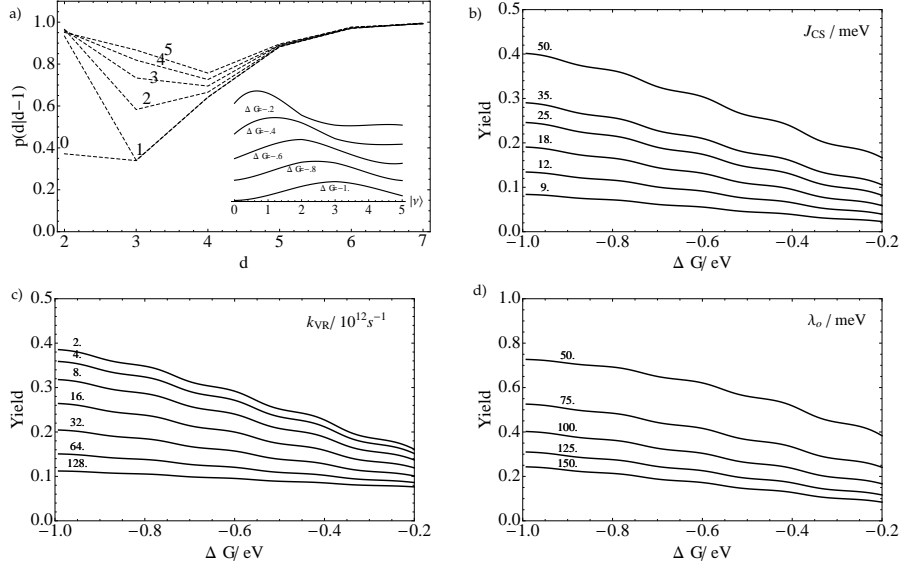


FIG. 2. Panel a) The conditional probability of the system reaching a certain distance  $d$  given that it has reached distance  $d - 1$  for different initial quanta of vibrational excitation. The inset shows the probability distribution of producing a certain number of quanta for various values of the driving force for exciton splitting. The curves are offset for clarity. The value of  $\Delta G$  in eV is shown below each curve. Panels b), c) and d) show the yield of charges at 5 nm as a function of the the driving force for charge separation  $\Delta G$  whilst changing the following parameters: b) the transfer integral for charge separation, c) the rate of internal relaxation, d) the outer sphere reorganization energy. Each curve is labelled by the value of the parameter used in that simulation.

exciton of such a molecule are rather similar in these classes of polymers, allowing some of the excess vibrational energy to be also used by the hole.

Two different forms of vibrational relaxation are allowed: via internal relaxation and via polaron hopping. Polaron hopping leads to a reduction in vibrational energy because at each hop some of the energy is left behind and because of the coupling to the classical bath. In the case when vibrational relaxation is slow compared to charge hopping a simple law for the number of hops necessary before thermalization was obtained, the number of hops is simply  $n = \log_2 \frac{\Delta G}{2\hbar\omega}$  where  $\Delta G$  is the driving force for charge separation, including the Coulomb attraction of a polaron pair. This leads to a thermalization distance  $d = a \log_2 \frac{\Delta G}{\hbar\omega}$ , where  $a$  is the separation between molecules.

Explicitly modeling charge transfer between vibrationally excited states allows high charge yields with fast recombination and explains the dependence of charge yield on the

driving force for exciton splitting. Improving charge transport improves charge generation because of more effective competition of charge separation with both charge recombination and vibrational relaxation. It must be noted that the model cannot reproduce the improvements in yields observed by Okhita and co-workers<sup>8</sup>. In their work they find that charge yields vary *exponentially* with driving force, whereas we find that it varies linearly. The fundamental reason for this discrepancy is that in this model at each hop the polaron must leave behind some of its vibrational energy. A possible way to overcome this feature is to assume that after exciton splitting a delocalised, hot charge transfer excitation is created. As it cools down this excitation would localise charges at potentially large distances. This situation would be tantamount to abandoning the assumptions of non-adiabacity and of loss of coherence at each hop. Future work will address this.

## ACKNOWLEDGMENTS

We acknowledge J. Nelson and J. Frost for useful discussion. The work was begun at Imperial College, London where it was supported by the Engineering and Physical Sciences Research Council. Support from the James Martin 21st Century School is also gratefully acknowledged.

## REFERENCES

- <sup>1</sup>K. Vandewal, K. Tvingstedt, A. Gadisa, O. Inganäs, and J. V. Manca, *Nat. Mater.* **8**, 904 (2009).
- <sup>2</sup>P. Peumans and S. R. Forrest, *Chem. Phys. Lett.* **398**, 27 (2004).
- <sup>3</sup>V. I. Arkhipov, E. V. Emelianova, and H. Bassler, *Phys. Rev. Lett.* **82**, 1321 (1999).
- <sup>4</sup>T. Offermans, S. C. J. Meskers, and R. A. J. Janssen, *Journ. Chem. Phys.* **119**, 10924 (2003).
- <sup>5</sup>J. Cabanillas-Gonzalez, T. Virgili, A. Gambetta, L. Lüer, G. Lanzani, T. D. Anthopoulos, and D. M. de Leeuw, *Phys. Rev. B* **75**, 045207 (2007).
- <sup>6</sup>S. H. Park, A. Roy, S. Beaupre, S. Cho, N. Coates, J. S. Moon, D. Moses, M. Leclerc, K. Lee, and A. J. Heeger, *Nat. Phot.* **3**, 297 (2009).

- <sup>7</sup>M. C. Scharber, D. Wuhlbacher, M. Koppe, P. Denk, C. Waldauf, A. J. Heeger, and C. L. Brabec, *Adv. Mat.* **18**, 789 (2006).
- <sup>8</sup>H. Ohkita, S. Cook, Y. Astuti, W. Duffy, S. Tierney, W. Zhang, M. Heeney, I. McCulloch, J. Nelson, D. D. C. Bradley, and J. R. Durrant, *JACS* **130**, 3030 (2008).
- <sup>9</sup>T. Offermans, S. C. J. Meskers, and R. A. J. Janssen, *Chem. Phys.* **308**, 125 (2005).
- <sup>10</sup>C. Groves, R. A. Marsh, and N. C. Greenham, *Journ. Chem. Phys.* **129** (2008).
- <sup>11</sup>M. Casalegno, G. Raos, and R. Po, *Journ. Chem. Phys.* **132**, 094705 (2010).
- <sup>12</sup>I. Montanari, A. F. Nogueira, J. Nelson, J. R. Durrant, C. Winder, M. A. Loi, N. S. Sariciftci, and C. Brabec, *APL* **81**, 3001 (2002).
- <sup>13</sup>D. Veldman, O. Ipek, S. C. J. Meskers, J. Sweelssen, M. M. Koetse, S. C. Veenstra, J. M. Kroon, S. S. van Bavel, J. Loos, and R. A. J. Janssen, *JACS* **130**, 7721 (2008).
- <sup>14</sup>I. Howard, R. Mauer, M. Meister, and F. Laquai, *JACS* **132**, 14866 (2010).
- <sup>15</sup>N. Kestner, J. Logan, and J. Jortner, *Journ Chem Phys* **78**, 2148 (1974).
- <sup>16</sup>H. Sumi and R. Marcus, *Journ Chem Phys* **84**, 4894 (1986).
- <sup>17</sup>J. Jortner and M. Bixon, *Journ. Chem. Phys.* **88**, 167 (1988).
- <sup>18</sup>J. Jortner, M. Bixon, T. Langenbacher, and M. E. Michel-Beyerle, *PNAS* **95**, 12759 (1998).
- <sup>19</sup>W. Q. Deng and W. A. Goddard, *Journ. Phys. Chem. B* **108**, 8614 (2004).
- <sup>20</sup>A. Troisi *Adv. Mat.* **19**, 2000 (2007).
- <sup>21</sup>J. Kirkpatrick, V. Marcon, J. Nelson, K. Kremer, and D. Andrienko *Phys. Rev. Lett.* **98** (2007).
- <sup>22</sup>V. Ruhle, J. Kirkpatrick, and D. Andrienko, *Journ. Chem. Phys.* **132**, 134103 (2010).
- <sup>23</sup>See Supplementary Material Document No. \_\_\_\_\_ for more detailed derivations. For information on Supplementary Material, see <http://www.aip.org/pubservs/epaps.html>
- <sup>24</sup>J. Klafter and R. Silbey, *Phys. Rev. Lett.* **44**, 55 (1980).
- <sup>25</sup>M. Linares, D. Beljonne, J. Cornil, K. Lancaster, J.-L. Brédas, S. Verlaak, A. Mityashin, P. Heremans, A. Fuchs, C. Lennartz, J. Idè, R. Mèreau, P. Aurel, L. Ducasse, and F. Castet, *Journ. Phys. Chem. C* **114**, 3215 (2010).
- <sup>26</sup>J. Szmytkowski, *Chem. Phys. Lett.* **470**, 123 (2009).
- <sup>27</sup>J. J. Kwiatkowski, J. M. Frost, and J. Nelson, *Nano Letters* **9**, 1085 (2009).
- <sup>28</sup>T. Clarke, A. Ballantyne, F. Jamieson, C. Brabec, J. Nelson, and J. Durrant, *Chem. Comm.* (2009).



## RECENT REPORTS

41/10	Optimal Error Estimates of a Mixed Finite Element Method for Parabolic Integro-Differential Equations with Non Smooth Initial Data	Goswami Pani Yadav
42/10	On the Linear Stability of the Fifth-Order WENO Discretization	Motamed Macdonald Ruuth
43/10	Four Bugs on a Rectangle	Chapman Lottes Trefethen
44/10	Mud peeling and horizontal crack formation in drying clay	Style Peppin Cocks
45/10	Binocular Rivalry in a Competitive Neural Network with Synaptic Depression	Kilpatrick Bressloff
46/10	A theory for the alignment of cortical feature maps during development	Bressloff Oster
47/10	All-at-Once Solution of Time-Dependent PDE-Constrained Optimisation Problems	Stoll Wathen
48/10	Possible role of differential growth in airway wall remodeling in asthma	Moulton Goriely
49/10	Variational Data Assimilation Using Targetted Random Walks	Cotter Dashti Robinson Stuart
50/10	A model for the anisotropic response of fibrous soft tissues using six discrete fibre bundles	Flynn Rubin Nielsen
51/10	STOCHSIMGPU Parallel stochastic simulation for the Systems Biology Toolbox 2 for MATLAB	Klingbeil Erban Giles Maini
52/10	Order parameters in the Landau-de Gennes theory - the static and dynamic scenarios	Majumdar
53/10	Liquid Crystal Theory and Modelling Discussion Meeting	Majumdar Mottram
54/10	Modeling the growth of multicellular cancer spheroids in a bioengineered 3D microenvironment and their treatment with an anti-cancer drug	Loessner Flegg Byrne Hall Moroney Clements Hutmacher McElwain

55/10	Scalar Z, ZK, KZK, and KP equations for shear waves in incompressible solids	Destrade Goriely Saccomandi
56/10	The Influence of Bioreactor Geometry and the Mechanical Environment on Engineered Tissues	Osborne ODEa Whiteley Byrne Waters
57/10	A numerical guide to the solution of the bidomain equations of cardiac electrophysiology	Pathmanathan Bernabeu Bordas Cooper Garny Pitt-Francis Whiteley Gavaghan
58/10	Particle-scale structure in frozen colloidal suspensions from small angle X-ray scattering	Spannuth Mochrie Peppin Wettlaufer
59/10	Spin coating of an evaporating polymer solution	Munch Please Wagner
60/10	Stochastic synchronization of neuronal populations with intrinsic and extrinsic noise	Bressloff Lai
61/10	Metastable states and quasicycles in a stochastic Wilson-Cowan model of neuronal population dynamics	Bressloff
62/10	Adsorption and desorption dynamics of citric acid anions in soil	Oburger Leitner Jones Zygalakis Schnepf Roose
63/10	A dual porosity model of nutrient uptake by root hairs soil	Zygalakis Kirk Jones Roose Wissuwa

**Copies of these, and any other OCCAM reports can be obtained**

**from:**

**Oxford Centre for Collaborative Applied Mathematics  
Mathematical Institute  
24 - 29 St Giles'  
Oxford  
OX1 3LB  
England  
[www.maths.ox.ac.uk/occam](http://www.maths.ox.ac.uk/occam)**